2.3 μm wavelength range digital Fourier transform on-chip wavelength monitor

Anton Vasiliev,[†] **Fabio Pavanello,**[†] **Muhammad Muneeb, and Günther Roelkens**

Photonics Research Group, Ghent University - imec, Technologiepark-Zwijnaarde 15, 9052 Ghent, Belgium.
Center for Nano- and Biophotonics, Technologiepark-Zwijnaarde 15, 9052 Ghent, Belgium.
anton.vasiliev@ugent.be

† These authors have equally contributed.

Abstract: We present a novel approach for on-chip wavelength monitoring based on a digital Fourier Transform spectrometer. We demonstrate 130 nm operational bandwidth and an accuracy of 100 pm in the 2.3 μm wavelength range.

OCIS codes: 120.6200, 130.3120.

1. Introduction

The rising interest in the mid-IR for spectroscopic sensing has fostered a large amount of work in recent years towards more compact, sensitive and cost-effective systems. One of the essential components of many sensing systems consists of a spectrometer, which allows to separate optical beams of different wavelengths. Common integrated spectrometer solutions are based on echelle gratings and arrayed waveguide gratings (AWGs). However, these approaches have an intrinsic limitation related to their footprint/resolution trade-off as for a given bandwidth the resolution scales inversely linearly with the device footprint [1]. This makes these spectrometers not very appealing for applications such as wavelength monitoring.

A novel approach, named digital Fourier Transform (dFT) spectrometer, that overcomes this limitation, has been recently proposed [2]. This approach is based on a cascade of Mach-Zehnder interferometers (MZIs), which are sequentially thermo-optically switched in a binary way (see Fig. 1(a)). Every MZI in the cascade is followed by a delay line pair and, depending on the switch state, light is sent to one of the delay lines. The MZI switches are inserted in a main MZI. At the device output light will interfere with an optical path delay (OPD) which is the difference between the optical paths of the 2 arms of the main MZI for a given configuration of switch states. In such case, the equivalent number of channels scales exponentially with the number of optical delay pairs [1]. The dFT spectrometer allows also to utilize only a single photodetector (PD), differently from classical AWG and echelle configurations with integrated detector arrays. This dFT approach has been recently demonstrated for spectrally broad input signals [1]. However, there are several applications such as wavelength monitoring in tunable laser systems or Raman spectroscopy which would benefit from systems able to identify only a very small set of discrete lines. Hence, we decided to investigate the dFT approach for spectrally sparse input signals. This choice allows to achieve a very broadband behavior because of the removal of artifacts, to reduce the computation time and to enhance the device robustness. Besides, the number of optical delay pairs may be reduced when using compressive sensing techniques without a loss in performance [3].

2. Design, fabrication and experimental results

The design is based on a 3-stage architecture as shown in Fig. 1(a) working around 2.3 μm wavelength because of its relevance for spectroscopic sensing applications [4]. The minimal OPD length $\Delta L = 10.825 \mu$m is obtained from [1]:

$$\delta\lambda \approx \frac{1}{2^N}\frac{\lambda^2}{n_g \Delta L} \tag{1}$$

where $\delta\lambda$ set to 2 nm is the channel bandwidth and $N = 6$ is the number of OPD pairs. Every stage ($k = 1, 2, 3$) has a top and a bottom arm with same spiral lengths $L_k = L_1 + 2^{2k-2}\Delta L$ where L_1 is a minimal length given by spiral design constraints. The increment of OPD for the top arm is $2^{2k-1}\Delta L$, while for the bottom arm it is $-2^{2k-2}\Delta L$ with respect to the common arm length of each delay line pair. Grating couplers are used for in/out light coupling. The design presents 2 outputs to integrate at a later stage a PD by e.g. flip-chip technology, while at the same time still being able to fiber-monitor the complementary output. The working principle consists of acquiring a calibration matrix A by scanning all the different 64 configurations of switch states as a function of the wavelength sampling/grid points. In such case the overall system can be represented with a linear relation $y = Ax$ where x is the unknown wavelength vector (weight of the different input wavelengths on the wavelength grid) and y is the

data recorded from the PD for the different switch configurations. Several techniques can be exploited to solve such problem depending on the signal input. By using the information on the sparse character of the input signal, the convex optimization problem can be solved using the efficient least absolute shrinkage and selection operator (LASSO) instead of more general methods such as the Moore-Penrose least-squares (LSQR) inverse. The latter has also disadvantages in terms of accuracy and operation bandwidth [1, 3]. The fabrication is based on a Silicon-
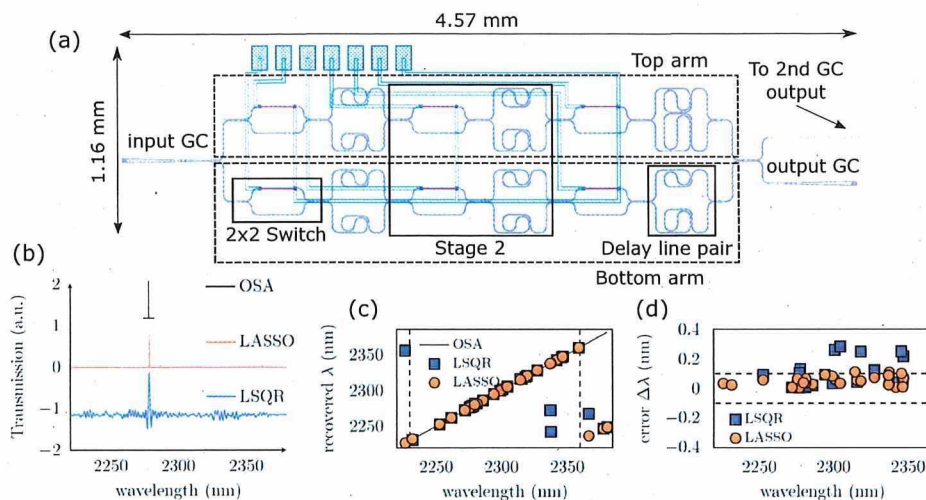

Fig. 1. Layout and performance of the 3-stage dFT spectrometer. (a) Layout view. A second complementary grating coupler output for later PD integration has been omitted for clarity. (b) Example of line retrieval compared to the OSA reference using 2 different methods: LSQR and LASSO. (c) Line retrieval positions using LASSO and LSQR methods. The latter provides outliers also in the operation bandwidth. (d) Error for the different methods, obtained by choosing random wavelengths.

on-Insulator (SOI) platform with 400 nm Si device layer thickness. A 180 nm partial etch is used to define rib waveguides and gratings by ebeam lithography and reactive ion etching. A SiO_2 layer is deposited to enable Ti-based heater fabrication above waveguides and related Ti/Au pads. The minimum feature dimensions of the dFT circuit are chosen such that all the fabrication can in principle be carried out using industry-standard silicon tools. The setup is based on a Yokogawa AQ6375 optical spectrum analyzer to record the spectrum and an IPG photonics SFTL-Cr-ZnS/Se laser as source. The chosen wavelength grid for the calibration was 500 pm. The accuracy of the spectral recovery was further increased by interpolating the calibration matrix on a finer 50 pm grid. Therefore the number of wavelength points was 3200 for a 160 nm span. Fig. 1(b) reports an example of wavelength recovery for the 2 methods (LASSO and LSQR). The LASSO method clearly shows a cleaner retrieved spectrum over the bandwidth of operation. We demonstrate correct wavelength recovery over the entire 130 nm bandwidth of the spectrometer (see Fig. 1(c)) and an accuracy of 100 pm is achieved as shown in Fig. 1(d). The LSQR method tends to produce consistently a larger error and thus it is not as suitable for sparse input signals.

3. Conclusions

We demonstrated a Si photonics dFT spectrometer for wavelength monitoring. We show an accuracy of 100 pm over a bandwidth of 130 nm for a device with 5.3 mm^2 footprint working in the 2.3 μm wavelength range.

References

1. D. M. Kita, B. Miranda, D. Favela, D. Bono, J. Michon, H. Lin, T. Gu, and J. Hu, "High-performance and scalable on-chip digital Fourier transform spectroscopy," Nature Communications 9, 1–7 (2018).
2. D. M. Kita, H. Lin, A. Agarwal, K. Richardson, I. Luzinov, T. Gu, and J. Hu, "On-Chip Infrared Spectroscopic Sensing: Redefining the Benefits of Scaling," IEEE Journal of Selected Topics in Quantum Electronics 23 (2017).
3. H. Podmore, A. Scott, P. Cheben, A. V. Velasco, J. H. Schmid, M. Vachon, and R. Lee, "Demonstration of a compressive-sensing Fourier-transform on-chip spectrometer," Optics Letters 42, 1440–1443 (2017).
4. R. Wang, S. Sprengel, A. Vasiliev, G. Boehm, J. Van Campenhout, G. Lepage, P. Verheyen, R. Baets, M.-C. Amann, and G. Roelkens, "Widely tunable 2.3 μm III-V-on-silicon Vernier lasers for broadband spectroscopic sensing," Photonics Research 6, 858 (2018).

| Joint | CLEO: Science & Innovations |

Tuesday 17:00–19:00

Joint

17:00–19:00
JTu4M • Symposium on Intense-field Nonlinear Optics & High Harmonic Generation in Nanoscale Materials II

JTu4M.1 • 17:00 `Invited`
Extreme nonlinear optics in two dimensional materials, Koichiro Tanaka[1]; [1]Kyoto Univ., Japan. We show recent progress of extreme non-linear optics in two dimensional materials. High-harmonic generation is confirmed not only in semiconductors but also metals under irradiation of mid-infrared femtosecond laser pulses. We found main mechanism changes according to the carrier doping status of the material.

JTu4M.2 • 17:30
Valleytronics on the subcycle timescale, Christoph P. Schmid[1], Stefan Schlauderer[1], Fabian Langer[1], Martin Gmitra[1], Jaroslav Fabian[1], Philipp Nagler[1], Tobias Korn[1], Christian Schüller[1], Peter Hawkins[2], Johannes T. Steiner[2], Ulrich Huttner[2], Markus Borsch[3], Benjamin Girodias[3], Stephan W. Koch[2], Mackillo Kira[3], Rupert Huber[1]; [1]Univ. of Regensburg, Germany; [2]Univ. of Marburg, Germany; [3]Univ. of Michigan, USA. Intense multi-terahertz waveforms drive electron-hole recollisions in monolayer WSe_2 and enable subcycle switching of the valley pseudospin. This dynamics manifests in high-odd-order side-band generation and opens the door to valleytronic protocols at optical clock rates.

JTu4M.3 • 17:45
Ultrafast laser pulse induced topological resonance in MoS2 monolayer, Seyyedeh Azar Oliaei Motlagh[1], Jhih-Sheng Wu[1], Vadym Apalkov[1], Mark Stockman[1]; [1]Georgia State Univ., USA. In MoS2 monolayer, we predict that a single oscillation femtosecond laser pulse with circular polarization creates a chiral distribution of conduction band electron population. This chirality is an effect of topological resonances in this semiconductor.

JTu4M.4 • 18:00
Carrier-Envelope Phase Detection with Arrays of Electrically Connected Bowtie Nanoantennas, Phillip D. Keathley[1], Yujia Yang[1], William Putnam[2], Praful Vasireddy[1], Franz Kärtner[1,3], Karl Berggren[1]; [1]Massachussetts Inst. of Technology, USA; [2]NG Next, Northrop Grumman Coorporation, USA; [3]Center for Free Electron Laser Science and DESY, Germany. We use arrays of electrically connected bowtie nanoantennas to detect the carrier-envelope phase of few-cycle optical pulses with noise performance close to the shot-noise limit. Our results pave the way towards low-cost, low-profile CEP monitoring and tagging.

CLEO: Science & Innovations

17:00–19:00
STu4N • Semiconductor-Based Optical Frequency Combs
Presider: Ben Williams; UCLA, USA

STu4N.1 • 17:00 `Tutorial`
Quantum Cascade Frequency Combs: Physics and Applications, Jérôme Faist[1]; [1]ETH Zurich, Switzerland. Quantum cascade lasers combs have demonstrated watt level emission over 100cm^{-1} in the mid-infrared, enabling new applications such as spectroscopy protein reaction dynamics. New insight in their physics has recently been gained.

Jérôme Faist has obtained his Ph.D from EPFL, and has worked successively at IBM Rüschlikon, AT&T Bell Laboratories and the University of Neuchatel. He now holds a chair in the physics department of the ETH Zurich.

STu4N.2 • 18:00
Optomechanical Control of the State of Chip-Scale Frequency Combs, David P. Burghoff[1,2], Ningren Han[1,3], Filippos Kapsalidis[4], Nathan Henry[5], Mattias Beck[4], Jacob Khurgin[5], Jerome Faist[4], Qing Hu[1]; [1]MIT, USA; [2]Univ. of Notre Dame, USA; [3]Google, USA; [4]ETH Zurich, Switzerland; [5]Johns Hopkins Univ., USA. Quantum cascade laser frequency combs have substantial potential in sensing. We show that by blending them with microelectromechanical comb drives, one can directly manipulate the dynamics of the laser and fully control the comb state.

17:00–19:00
STu4O • Infrared Photonics & Applications
Presiders: Nan Zhang; State University of New York at Buffalo, USA
Haomin Song; State University of New York at Buffalo, USA

STu4O.1 • 17:00
Compact, ultra-tunable InGaSb/AlGaAsSb Si external cavity laser at the Mid-Infrared (MIR), Sia J. Brian[1], Wanjun Wang[1], Zhongliang Qiao[1], Xiang Li[1], Xin Guo[1], Jin Zhou[1], Zecen Zhang[1], Callum Littlejohns[2,1], Chongyang Liu[1], Graham T. Reed[2,1], Hong Wang[1]; [1]Nanyang Technological Univ., Singapore; [2]Optoelectronics Research Centre, Univ. of Southampton, UK. We present the first MIR hybrid Si external cavity laser with a tunable range below the 2 μm mark. To the best of our knowledge, we have achieved the largest tunable range of 66 nm (1881-1947 nm) near the 2 μm waveband in silicon photonics.

STu4O.2 • 17:15
Withdrawn

STu4O.3 • 17:30
Photonic Integrated Si_3N_4Ultra-Large-Area Grating Waveguide MOT Interface for 3D Atomic Clock Laser Cooling, Nitesh Chauhan[1], Debapam Bose[1], Matthew Puckett[2], Renan Moreira[1], Karl Nelson[2], Daniel Blumenthal[1]; [1]Univ. of California, Santa Barbara, USA; [2]Honeywell, USA. We describe a silicon nitride (Si_3N_4) photonic integrated circuit (PIC) designed to deliver non-diverging 780nm free-space optical cooling beams to an [87]Rb atomic magneto optic trap (MOT) via fiber coupled ultra-large-area 3.88mm x 2.08mm gratings.

STu4O.4 • 17:45
2.3 μm Wavelength Range Digital Fourier Transform on-Chip Wavelength Monitor, Anton Vasiliev[1,2], Fabio Pavanello[1,2], Muhammad Muneeb[1,2], Gunther Roelkens[1,2]; [1]Photonics Research Group, Ghent Univ. - imec, Belgium; [2]Center for Nano- and Biophotonics, Belgium. We present a novel approach for on-chip wavelength monitoring based on a digital Fourier Transform spectrometer. We demonstrate 130 nm operational bandwidth and an accuracy of 100 pm in the 2.3 μm wavelength range.

STu4O.5 • 18:00 `Invited`
Ge-rich SiGe Photonic Circuits for Mid IR spectroscopy, Delphine Marris-Morini[1]; [1]Universite de Paris-Sud, France. Ge-rich SiGe photonic circuits have been used to demonstrate a whole set of devices in the mid-IR, such as interferometers, spectrometers or cavities. The perspectives towards the realization of optical sources will be also presented.